Liquid Crystals
Publication details, including instructions for authors and subscription information:
http://www.informaworld.com/smpp/title~content=t713926090

Response speed of in-plane switching mode liquid crystal displays

Guan Rong-Hua[a]; Kang Wen-Xiu[a]; Sun Yu-Bao[b]
[a] Department of Applied physics, North China Electric Power University, Baoding 071003, PR China [b] Department of Applied Physics, Hebei University of Technology, Tianjin, PR China

To cite this Article Rong-Hua, Guan , Wen-Xiu, Kang and Yu-Bao, Sun(2007) 'Response speed of in-plane switching mode liquid crystal displays', Liquid Crystals, 34: 4, 467 — 471
To link to this Article: DOI: 10.1080/02678290701251419
URL: http://dx.doi.org/10.1080/02678290701251419

Liquid Crystals, Vol. 34, No. 4, April 2007, 467–471

Taylor & Francis
Taylor & Francis Group

Response speed of in-plane switching mode liquid crystal displays

GUAN RONG-HUA*†, KANG WEN-XIU† and SUN YU-BAO‡
†Department of Applied physics, North China Electric Power University, Baoding 071003, PR China
‡Department of Applied Physics, Hebei University of Technology, Tianjin, 300130, PR China

(*Received 26 July 2006; in final form 28 November 2006; accepted 28 November 2006*)

The response speed of in-plane switching mode liquid crystal displays with three initial director configurations—homogeneous, twisted nematic and 180° super twisted nematic—was investigated via simulations. These simulations studied the relationship between the change in the optical axis and the optical transmission in the three configurations, allowing us to calculate the optical response times. The time-dependent change in the director was calculated using the Erickson–Leslie equations and these two results combined. These results predict that the response time during both the rise and decay periods of a super twist cell is about four times faster than the other two configurations.

1. Introduction

Liquid crystals are widely studied because of their promising possibilities in display applications [1]. In-plane switching (IPS) mode liquid crystal displays (LCDs) are used in superior quality displays because of their excellent viewing angle, high contrast ratio and low colour shift [2–4]. However, the dynamic response speed of this display mode is slow compared with other modes [5–8]. Several methods have been proposed for the solution of this problem. By increasing the rubbing angle between the rubbing direction and electrodes up to 30°, the response speed of the rise period can be three times faster than that for conventional 10° rubbing angle [6], but the decay period remains unchanged. The IPS mode with twisted nematic (TN) configuration can also achieve a faster response speed in the rise period, but has no improvement in the decay period [9]. To improve the response speed during both rise and decay periods, polymer-stabilized IPS has been proposed [10], but light leakage is unavoidable due to scattering in the off-state. To improve the response speed during both the rise and decay periods based on the driving circuit, the over-driving circuit method has been proposed [11]. However, such a driving technology is quite complicated to implement. The wide viewing angle characteristic and low colour shift can be held in each solution.

In this paper, we theoretically analyse the dynamic response process of IPS mode LCDs with three different configurations: homogeneous alignment, TN and 180° super twisted nematic (STN). Simulation results show that the response speed of the IPS-STN mode is about four times faster than optimal IPS and IPS-TN modes during both rise and decay periods. Other optical characteristics, such as viewing angle and colour shift, of this mode with film compensation will be discussed elsewhere.

*Corresponding author. Email: ronghua_guan@sohu.com

2. Theory and results

Figure 1 illustrates the geometry of the IPS mode LCD with three configurations: homogeneous alignment, TN and 180° STN. Hereafter, we assume that the in-plane electric field is uniform throughout the LC layer, and that LC molecules are switched only within the plane parallel to the substrates. To analyse the dynamic transition process, the Erickson–Leslie equation is used to calculate the LC director reorientation process [12, 13]. When backflow and inertial effects are ignored, the dynamics of the LC director reorientation is described

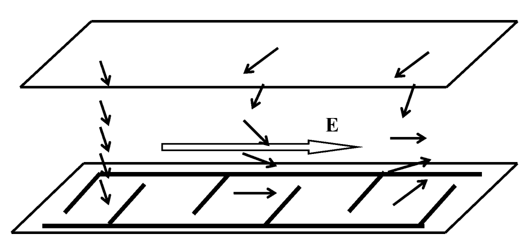

Figure 1. Geometry of the three configurations: homogeneous (left), TN (middle) and STN (right). The applied electric field is parallel to the substrates.

Liquid Crystals
ISSN 0267-8292 print/ISSN 1366-5855 online © 2007 Taylor & Francis
http://www.tandf.co.uk/journals
DOI: 10.1080/02678290701251419

by the following equation [14]

$$\gamma \frac{\partial \phi}{\partial t} = K_2 \frac{\partial^2 \phi}{\partial z^2} + \varepsilon_o |\Delta\varepsilon| \mathbf{E}^2 \sin\phi \cos\phi \qquad (1)$$

Where $\mathbf{E}$ is the in-plane electric field, ϕ is the rotation angle of LC director, ε_o is the vacuum dielectric constant, γ is the rotational viscosity, K_2 is the twist elastic constant, and $\Delta\varepsilon$ is the dielectric anisotropy of the LC mixture. In IPS-TN and IPS-STN modes, the chiral term in the dynamic equation has little effect on reorientation time and can be ignored if the pretilt angle is small [15]. In our simulation, the anchoring condition at the interface of LC and substrate is assumed to be strong, and the pretilt angle is assumed to be zero. The polarization axis of incident light is parallel to the rubbing direction in the adjacent substrate. For the IPS mode with homogeneous alignment, the transmission of an LCD with crossed polarizers is given by

$$T = \sin^2(2\alpha)\sin^2\left[\frac{\pi d \Delta n(\phi, \lambda)}{\lambda}\right]. \qquad (2)$$

Here, d is the cell gap, λ is the wavelength of incident light and Δn is the LC birefringence; α symbolizes the change in the optical axis of the LC layer under an applied electric field and is described in next paragraph. For IPS-TN and IPS-STN modes, a compensation film must be used to achieve a good dark-state at off-state and high transmission at on-state, so the transmission equation becomes complicated, but the compensation term can be regarded as a constant [16]. Satake *et al.* show that the birefringence Δn varies with λ and ϕ, and its effect on transmission is analysed for conventional IPS mode [16]. These results show that the second factor has no effect on the on-state voltage and little effect on the transmission, because the LC molecules rotate in the plane of the substrate, and the electro-optical transmission curve depends mainly on α. The equation is also applied in IPS-TN and IPS-STN mode because of the same rotational behavior of the LC molecules. So equation (2) can be rewritten as $T \propto \sin^2(2\alpha)$ for the three modes.

The angle between the effective optical axis of LC layer and the polarization axis of incident light is zero for optimal IPS mode and $\pi/4$ for TN mode when the electric field is zero. For 180° IPS-STN mode, the LC layer can be regarded as the combination of double TN configurations with the effective optical axis angles being $\pi/4$ and $3\pi/4$ without an applied electric field. Under an applied electric field, the change in the optical axis of the LC layer is defined as $\alpha = \frac{1}{d}\int_0^d [\phi(z) - \Phi]\mathrm{d}z$ (IPS mode) where Φ is the rubbing angle; $\alpha = \frac{1}{d}\int_0^d [\phi(z) - \frac{\pi}{4}]\mathrm{d}z$ (IPS-TN mode); $\alpha_1 = \frac{2}{d}\int_0^{\frac{d}{2}} [\phi(z) - \frac{\pi}{4}]\mathrm{d}z$ (lower half) and $\alpha_2 = \frac{2}{d}\int_{\frac{d}{2}}^{d} [\phi(z) - \frac{3\pi}{4}]\mathrm{d}z$ (upper half) for the IPS-STN mode. Here $\alpha_1 = -\alpha_2 = \alpha$, thus we can use α to denote the change of optical axis in the IPS-STN mode because of the anti-symmetric configurations about the middle layer.

For the IPS mode with homogeneous alignment, the rise time and decay time for the switching process are expressed as [6]:

$$\tau_{\mathrm{rise}} = \frac{\gamma}{\varepsilon_o |\Delta\varepsilon| \mathbf{E}^2 \left[\cos(2\Phi)\frac{\sin(2\alpha)}{2\alpha} + \sin(2\Phi)\frac{\cos(2\alpha)}{2\alpha}\right] - \frac{\pi^2}{d^2}K_2} \qquad (3a)$$

$$\tau_{\mathrm{decay}} = \frac{\gamma d^2}{\pi^2 K_2}. \qquad (3b)$$

They are defined as the LC director reorientation times; that is, the mean time for the normalized optical axis to change from $1/e$ to 1 (rise process) and from 1 to $1/e$ (decay process), respectively. For IPS-TN and IPS-STN modes, we can not obtain analytical results of the reorientation time, but can get numerical results from equation (1).

The director arrangement at arbitrary time can be calculated by using equation (1) after the electric field is applied or removed. The change in the effective optical axis of LC layer (α) can then be calculated. We depict the time-dependent normalized change, $\alpha(t)/\alpha(t \to \infty)$, of the effective optical axis in figures 2–4 for the three modes.

Figures 2–4 show the normalized change of the optical axis as a function of time for various electric fields. Figure 2 illustrates the optimized IPS mode with 30° rubbing angle, figure 3 the IPS-TN geometry, and figure 4 the IPS-STN geometry. The various curves showing different rise times correspond to different electric fields, which vary from 0.1 to 1 V μm^{-1} in steps of 0.1 V μm^{-1} in figure 2, and 0.1 to 2 V μm^{-1} in figures 3 and 4. For convenience, the same parameters

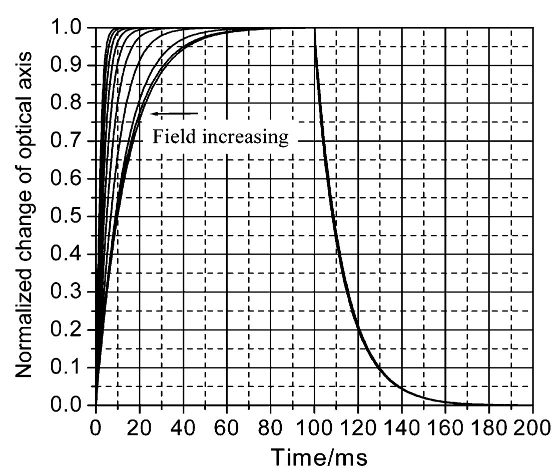

Figure 2. Normalized change in optical axis for the optimal IPS mode LCD with 30° rubbing angle.

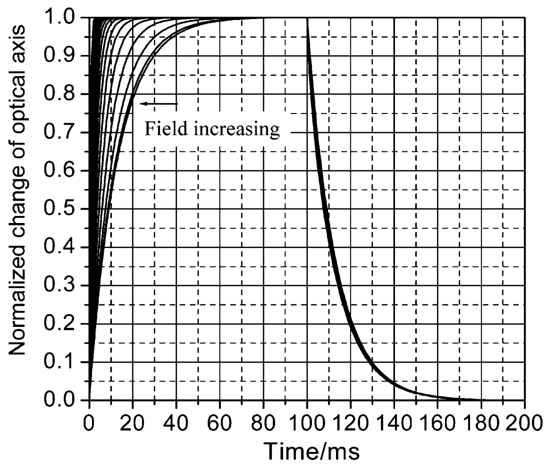

Figure 3. Normalized change in optical axis for the IPS-TN mode LCD.

are used in each simulation: $d=3\,\mu m$, $\Delta\varepsilon=7.8$, $K_2=7\,pN$ and $\gamma=0.1\,Pa\,s$. From figures 2 and 3, the response speed of the IPS-TN mode is not faster than that of the optimal IPS mode. Figure 4 shows that the response speed of the IPS-STN mode is faster than that of optimal IPS and IPS-TN modes. The optical response time can be obtained from these figures by using a relationship between normalized changes of the optical axis and optical transmission.

The normalized change in optical transmission, corresponding to normalized change in optical axis, is defined as follows

$$T = \frac{\sin^2[2(x\alpha)]}{\sin^2(2\alpha)} \tag{4}$$

where, x is termed the normalized coefficient ($0 \leqslant x \leqslant 1$), and symbolizes the normalized change in the optical axis. The time taken for normalized transmission to change from 0.1 to 0.9 (rise process) and from 0.9 to 0.1 (decay process) is defined as the optical response time. Using equation (4), the normalized changes in optical axis corresponding to the normalized transmission of 0.1 or 0.9 for different changes in optical axis are shown in figure 5. The normalized changes in optical axis for $T=0.1$ are 0.32 as $\alpha \to 0$, and 0.2 as $\alpha \to \pi/4$. The corresponding values for $T=0.9$ are 0.95 and 0.8. The change in optical axis under various applied electric fields is shown in figure 6.

The optical response times are less than 35 ms (rise time) and about 16–18 ms (decay time) for optical IPS and IPS-TN modes (from figures 2 and 3), and less than 9 ms (rise time) and ~4 ms (decay time) for the IPS-STN mode (from figure 4). The response time for the IPS-

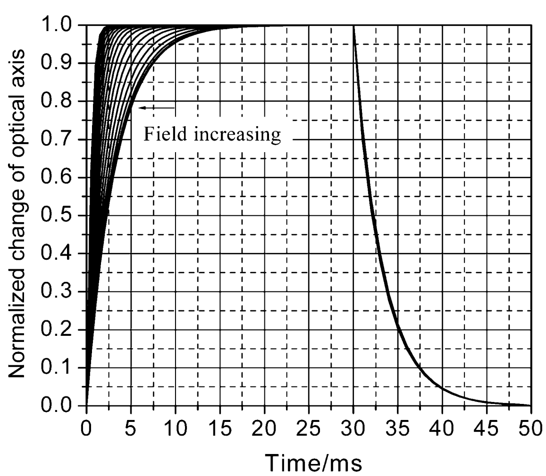

Figure 4. Normalized change in optical axis for the IPS-STN mode LCD.

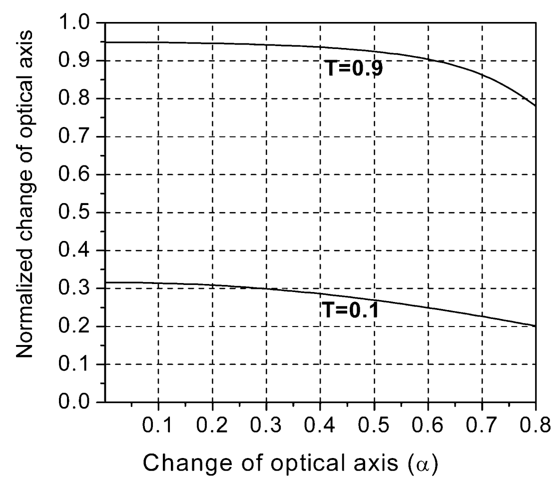

Figure 5. Normalized change in optical axis with change in the optical axis (α) at the normalized change in optical transmission of 0.1 and 0.9.

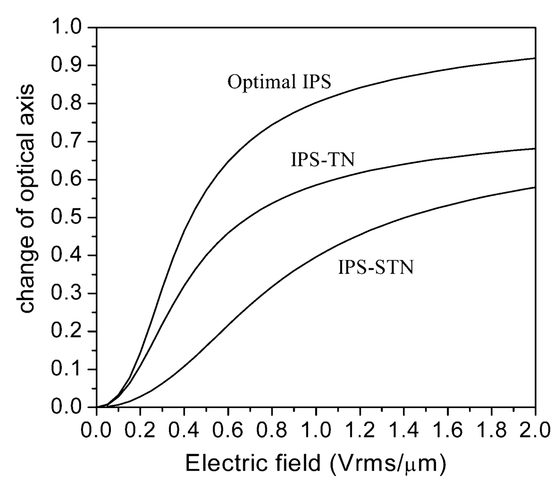

Figure 6. Change in optical axis with variation of applied electric field for the three modes.

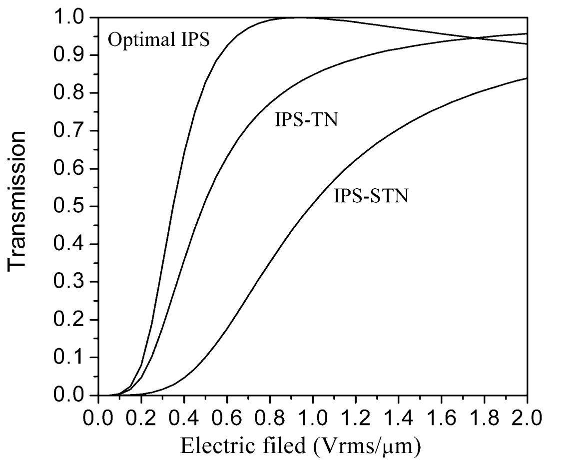

Figure 7. Voltage-dependent transmission of the three modes by using $T = \sin^2(2\alpha)$.

STN mode is about a quarter that in IPS-TN or optimal IPS modes. In the 180° IPS-STN mode, liquid crystal molecules in the middle layer do not rotate under the external electric field. Therefore, the middle layer is equivalent to a strongly anchoring boundary layer. Due to such an unchanged boundary layer, the 180° IPS-STN cell is divided into two effective thinner cells, each with half of the original cell gap [17]. Its response times are improved approximately four-fold, being proportional to the square of the cell gap. This is very important in the design of superior quality displays.

3. Optical response speed

In figure 7, the voltage-dependent steady state normalized transmission of the three modes is shown by using $T = \sin^2(2\alpha)$. The saturation electric field of the optimal IPS mode, corresponding to the maximum transmission, is $\sim 1.0\,V_{rms}\,\mu m^{-1}$. The transmission decreases as the electric field increases when it is larger than $1.0\,V_{rms}\,\mu m^{-1}$. The transmissions of the IPS-TN and

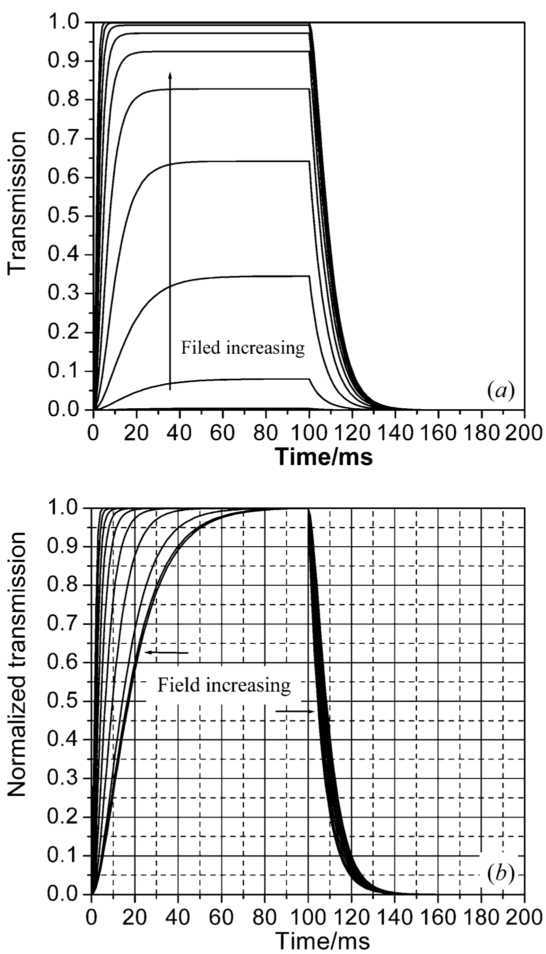

Figure 8. (a) Time-dependent transmission and (b) time-dependent normalized transmission, in optimal IPS mode with 30° rubbing angle.

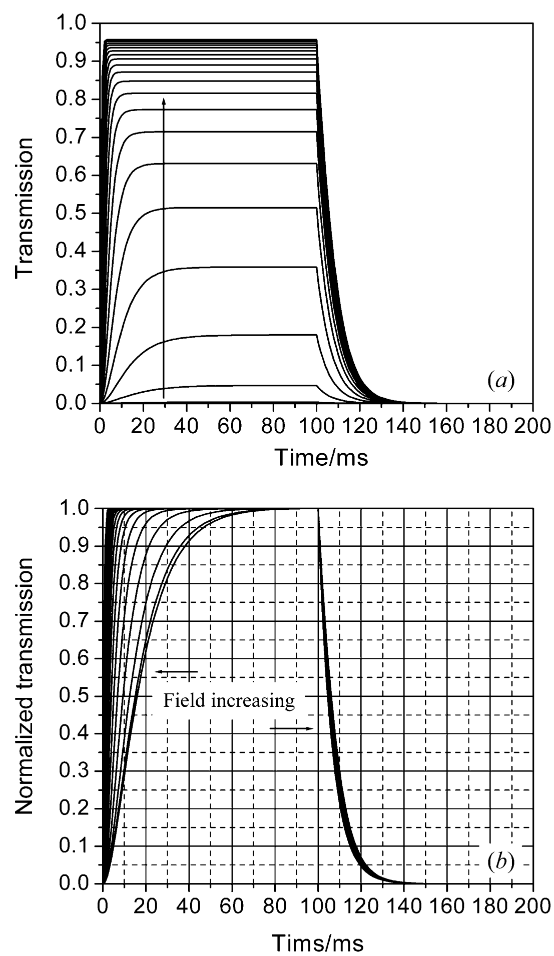

Figure 9. (a) Time-dependent transmission and (b) time-dependent normalized transmission, in IPS-TN mode.

IPS-STN modes are lower than that of the optimal IPS mode, and have no maximum because the change in optical axis can only tend to $\pi/4$, but can not reach it except when the applied electric field is infinite or the condition at the interface between LC and substrate is weak anchoring. The transmission can be improved by using compensation film [18].

In figures 8 (*a*)–10 (*a*) time-dependent transmissions obtained by using $T = \sin^2(2\alpha)$ are shown for increasing electric field. Figures 8 (*b*)–10 (*b*) show time-dependent normalized transmissions obtained by using $T = \frac{\sin^2[2\alpha(t)]}{\sin^2[2\alpha(t \to \infty)]}$ for the three modes under increasing applied electric field. The change in applied electric field is the same as that in figures 2–4. The optical response times are easily obtained from figures 8 (*b*)–10 (*b*). The decay time is not a constant and increases slowly as the applied electric field increases. This result agrees with experiment results [9]. The results of optical response times (rise and decay times) are the same as those in the above section.

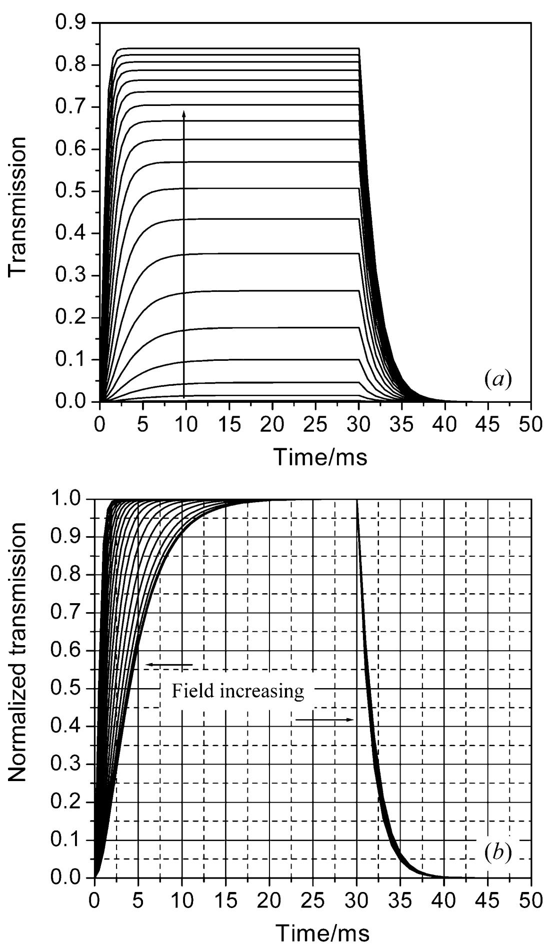

Figure 10. (*a*) Time-dependent transmission and (*b*) time-dependent normalized transmission, in IPS-STN mode.

4. Conclusion

We analysed the response speed of the in-plane switching mode LCD with three different initial configurations: homogeneous alignment, TN and 180° STN. Based on our simulation results, not only response speed is affected by the rubbing angle and cell gap, but also by the twist angle of the LC layer. Among these three configurations, the IPS-STN mode LCD with 180° super twist configuration can improve the optical response speed approximately four-fold during both rise and decay periods.

Acknowledgement

This project was supported by the Natural Science Foundation of Hebei Province (Grant No. A2006000675), the Doctoral Foundation of Hebei Province (Grant No. 05547001D-3), the Key Project Foundation of North China Electric Power University, China (Grant No. 200513002), and the Key Construction Project of Hebei Province University, China.

References

[1] S.T. Wu, D.K. Yang. *Reflective Liquid Crystal Displays*. Chichester, Wiley (2001).
[2] R. Kiefer, B. Weber, F. Windsceid, G. Baur. In Proceedings of the 12th International Display Research Conference, Hiroshima, Japan, p.547 (1992).
[3] M. Oh-e, K. Kondo. *Appl. Phys. Lett.*, **67**, 3895 (1995).
[4] M. Oh-e, M. Yoneya, K. Kondo. *J. appl. Phys.*, **82**, 528 (1997).
[5] M. Oh-e, K. Kondo. *Liq. Cryst.*, **22**, 379 (1997).
[6] Y. Sun, Z. Zhang, H. Ma, X. Zhu, S.T. Wu. *Appl. Phys. Lett.*, **81**, 4907 (2002).
[7] Y. Sun, Z. Zhang, H. Ma, X. Zhu, S.T. Wu. *J. appl. Phys.*, **93**, 3920 (2003).
[8] Y. Sun, H. Ma, Z. Zhang, S.T. Wu. *J. appl. Phys.*, **92**, 1956 (2002).
[9] S. Oka, K. Kobayashi, Y. Iwamoto, Y. Toko, M. Kimura, T. Akahane. *Jpn. J. appl. Phys.*, **42**, 7445 (2003).
[10] M.J. Escuti, C.C. Bowley, G.P. Crawford, S. Zumer. *Appl. Phys. Lett.*, **75**, 3264 (1999).
[11] I.J. Chung, C.H. Oh, H.C. Choi. In Proceeding of the 8th Asian Symposium on Information Display, Nanjing, China, p.42 (2004).
[12] J.L. Erickson. *Trans. Soc. Rheol.*, **5**, 23 (1961).
[13] F.M. Leslie. *Arch. Ration. Mech. Anal.*, **28**, 265 (1968).
[14] S. Chandrasekhar. *Liquid Crystals* 2nd Edn, Cambridge University Press, (1992).
[15] Y. Sun, Z. Zhang, H. Ma. *Chin. J. comp. Phys.*, **18**, 447 (2001).
[16] T. Satake, T. Nishioka, T. Saito, T. Kurata. *Jpn. J. appl. Phys.*, **40**, 195 (2001).
[17] Y. Sun, H. Ma, Z. Zhang, X. Zhu, S.T. Wu. *Appl. Phys. Lett.*, **89**, 041110 (2006).
[18] S. Oka, K. Kobayashi, Y. Iwamoto, Y. Toko, M. Kimura, T. Akahane. *Jpn. J. appl. Phys.*, **43**, 3443 (2004).